Monthly Notices of the ROYAL ASTRONOMICAL SOCIETY

MNRAS **469,** 4428–4436 (2017) doi:10.1093/mnras/stx1014
Advance Access publication 2017 April 27

Understanding the non-linear clustering of high-redshift galaxies

Charles Jose,[1,2]★ Carlton M. Baugh,[1] Cedric G. Lacey[1] and Kandaswamy Subramanian[3]

[1]*Institute for Computational Cosmology, Department of Physics, University of Durham, South Road, Durham DH1 3LE, UK*
[2]*Department of Physics, SB College, Changanassery, Kottayam 686101, India*
[3]*IUCAA, Post Bag 4, Pune University Campus, Ganeshkhind, Pune 411007, India*

Accepted 2017 April 25. Received 2017 April 25; in original form 2017 February 1

ABSTRACT

We incorporate the non-linear clustering of dark matter haloes, as modelled by Jose et al. into the halo model to better understand the clustering of Lyman break galaxies (LBGs) in the redshift range $z = 3$–5. We find that, with this change, the predicted LBG clustering increases significantly on quasi-linear scales ($0.1 \leq r/h^{-1}\,\mathrm{Mpc} \leq 10$) compared to that in the linear halo bias model. This, in turn, results in an increase in the clustering of LBGs by an order of magnitude on angular scales $5 \leq \theta \leq 100$ arcsec. Remarkably, the predictions of our new model on the whole remove the systematic discrepancy between the linear halo bias predictions and the observations. The correlation length and large-scale galaxy bias of LBGs are found to be significantly higher in the non-linear halo bias model than in the linear halo bias model. The resulting two-point correlation function retains an approximate power-law form in contrast with that computed using the linear halo bias theory. We also find that the non-linear clustering of LBGs increases with increasing luminosity and redshift. Our work emphasizes the importance of using non-linear halo bias in order to model the clustering of high-z galaxies to probe the physics of galaxy formation and extract cosmological parameters reliably.

Key words: galaxies: haloes – galaxies: high-redshift – galaxies: statistics – cosmology: theory.

1 INTRODUCTION

The halo model of large-scale structure is a successful formalism for predicting and interpreting the clustering of dark matter haloes and the galaxies associated with them (Cooray & Sheth 2002). In the halo model the galaxy correlation function ($\xi_{\rm g}(r)$) is the sum of two terms, the one-halo term and the two-halo term. The one-halo term accounts for the contributions to the clustering from galaxy pairs residing within the same dark matter halo and dominates the galaxy clustering on small scales. Since visible galaxies are formed in dark matter haloes and subhalos, the shape of the one-halo term is determined by dark matter halo substructure (Berlind & Weinberg 2002). The two-halo term, that accounts for the correlation between galaxies residing in distinct haloes, dominates the clustering of galaxies on scales larger than their typical halo virial radius. The crucial component of the two-halo term is the halo bias that determines how dark matter haloes trace the dark matter on large scales (Kaiser 1984; Cole & Kaiser 1989; Bond et al. 1991).

Interestingly, the predicted galaxy correlation functions at low redshifts have an almost power-law form ($\xi_{\rm g}(r) = (r/r_0)^{-\gamma}$), with a subtle feature on scales ($r \sim 1$–$2\,h^{-1}$ Mpc) corresponding to the transition from the one-halo to the two-halo term (Berlind & Weinberg 2002; Kravtsov et al. 2004; Zehavi et al. 2004; Watson, Berlind & Zentner 2011). The halo model has been highly successful in explaining many low-redshift clustering measurements over a wide range of galaxy–galaxy separations (Zehavi et al. 2004, 2005; Conroy, Wechsler & Kravtsov 2006; Zheng et al. 2009; Zehavi et al. 2011; Guo et al. 2013; Parejko et al. 2013). The clustering measurements for high redshift ($3 \leq z \leq 5$) galaxy samples shows stronger departures from a power law, particularly around the transition from the one-halo to two-halo terms (Ouchi et al. 2005; Lee et al. 2006; Hildebrandt et al. 2009; Cooke, Omori & Ryan-Weber 2013). Nevertheless, the measured galaxy correlation functions in this redshift range are typically approximated as a power law (Kashikawa et al. 2006; Savoy et al. 2011; Bian et al. 2013; Durkalec et al. 2015; Harikane et al. 2016; Ishikawa et al. 2016; Park et al. 2016). Interestingly, the measured clustering of galaxies retains an approximate power-law form even at a higher redshift ∼7 (Barone-Nugent et al. 2014).

However, models of the clustering of very high redshift ($z \geq 3$) galaxies using the standard halo model predict a much stronger deviation from a power law than is suggested by the observations (Ouchi et al. 2005; Lee et al. 2009; Jose et al. 2013b). In particular,

★ E-mail: charlesmanimala@gmail.com

Jose et al. (2013b; hereafter J13) point out that the predicted angular clustering of Lyman break galaxies (LBGs) on angular scales $10 \leq \theta \leq 100$ arcsec is lower than the observed clustering by an order of magnitude. These angular scales (corresponding to comoving length of 0.5–10 Mpc) are bigger than the virial radii of the typical dark matter haloes at that redshift, but smaller than scales where the linear theory is valid, and therefore referred to as quasi-linear scales. On these scales, the significant contribution to the galaxy clustering comes from the two-halo term. J13 modelled the two-halo term in this regime using the large-scale linear halo bias (Mo & White 1996; Sheth & Tormen 1999; Tinker et al. 2010). At $z = 0$, deviations from the linear halo bias approximation on quasi-linear scales are found to be of the order of only a few per cent (Tinker et al. 2005; van den Bosch et al. 2013). However, such a weak scale dependence of the halo bias is not sufficient to explain the discrepant clustering strength of high-z LBGs. To summarize, the halo model predictions of high-z LBG clustering that use linear halo bias show substantial departures from a power law and underpredict the observed correlation functions on quasi-linear scales (J13).

Here, we investigate whether considering the scale-dependent non-linear bias of high-z dark matter haloes on quasi-linear scales removes the tension between the halo model predictions and the observed LBG clustering. For this, we use the model introduced by Jose, Lacey & Baugh (2016; hereafter J16), who showed that the linear halo bias approximation breaks down on quasi-linear scales at high-z. In particular, they showed that the scale dependence of non-linear halo bias in this region is much stronger at high-z compared to low-z.

There are previous works, especially at low redshifts ($z \sim 0$), which show the importance of using a weakly scale-dependent non-linear halo bias on quasi-linear scales for a better comparison of theoretical predictions with observed data (Cooray 2004; Zehavi et al. 2004; van den Bosch et al. 2013). The consequences of the non-linear clustering of mini-haloes on quasi-linear scales during the cosmic dark ages ($z \geq 6$) and the implications for future observations of this epoch are discussed by Iliev et al. 2003 and Reed et al. 2009. Here, we focus on the clustering of galaxies in the redshift range 3–5, thereby bridging the gap between these two distinct epochs in the cosmic history. This is the first work, to our knowledge, that uses the non-linear bias of dark matter haloes on quasi-linear scales to better understand the measured clustering of LBGs at $3 \leq z \leq 5$.

The organization of this paper is as follows. In the next section, we present our model for the halo occupation distribution (HOD) and the non-linear clustering of high-z dark matter haloes. In Section 3, we compute the two-point spatial and angular correlation functions of LBGs and compare them with observations. We present our conclusions in the final section. For all calculations, we adopt a flat Λ cold dark matter universe with cosmological parameters consistent with the 9-yr *Wilkinson Microwave Anisotropy Probe* observations (Hinshaw et al. 2013). Accordingly, we assume a Hubble parameter $h = 0.70$, a baryon density $\Omega_{\rm b} = 0.0463$, cold dark matter density $\Omega_{\rm c} = 0.233$, density of massive neutrinos $\Omega_{\nu} = 0.0$, fluctuation normalization $\sigma_8 = 0.821$ and spectral index $n_{\rm s} = 0.972$ (where $\Omega_{\rm i}$ is the background density of any species 'i' in units of critical density $\rho_{\rm c}$).

2 THE CLUSTERING OF HIGH-REDSHIFT LBGs

Here, we discuss the two key components of our galaxy clustering model: (i) the HOD; and (ii) the model for the non-linear clustering of dark matter haloes.

2.1 The halo occupation distribution

The HOD is an important ingredient for computing the two-point correlation function of any galaxy sample. The HOD gives mean number of galaxies of a given type in a dark matter halo of mass M and is usually presented in a parametrized form (Seljak 2000; Bullock, Wechsler & Somerville 2002; Hamana et al. 2004; Kravtsov et al. 2004; Zehavi et al. 2005; Conroy et al. 2006; Hamana et al. 2006). Galaxy clustering can be calculated by combining the HOD with dark matter clustering, dark matter halo abundance, halo bias and the halo density profile.

In order to compute the clustering of LBGs selected to be brighter than some luminosity threshold, we use the HOD computed using the galaxy formation model of J13 for illustrative purposes (see also Samui, Srianand & Subramanian 2007). In this model, each dark matter halo can host a central galaxy and satellite galaxies. The central galaxy is put at the centre of the halo and satellite galaxies are distributed around the central galaxy following the dark matter density profile. The satellite galaxy occupation, which is the mean number of satellite galaxies in a dark matter halo, is computed using the conditional or progenitor mass function (Lacey & Cole 1993; Cooray & Sheth 2002). J13 then incorporate a physically motivated model for the total star formation rate in a dark matter halo to compute the ultravoilet (UV) luminosity of the LBGs hosted by the halo. The parameters of the model are constrained by fitting the observed UV luminosity functions of LBGs from Bouwens et al. (2007), Reddy et al. (2008) and Bouwens et al. (2012). Thus, J13 constrains the relation between the UV luminosity and halo mass of high-z LBGs from which the HOD of LBGs brighter than a given luminosity is computed.

The mean number of LBGs brighter than apparent AB magnitude m inside a dark matter halo of mass M, separated into central and satellite components, can be written as

$$N_{\rm g}(M, m, z) = N_{\rm cen}(M, m, z) + N_{\rm s}(M, m, z). \quad (1)$$

Here, $N_{\rm cen}(M, m, z)$ and $N_{\rm s}(M, m, z)$ are, respectively, the average number of central and satellite galaxies in a halo of mass M, satisfying the luminosity threshold condition. The separation of the HOD of LBGs into central and satellite components is crucial for computing the clustering (Kravtsov et al. 2004; Zheng et al. 2005; Cooray & Ouchi 2006; Conroy et al. 2006). Further details about the computation of the central and satellite contribution to the HOD can be found in J13.

In Fig. 1 (same as fig. 7 in J13), the average occupation number of LBGs is plotted as function of the mass of the parent halo computed using the model of J13 for $z = 3$–5 and for three apparent magnitude thresholds, for which clustering measurements are available (Hildebrandt et al. 2009). Also shown is $N_{\rm cen}(M, m, z)$, the mean occupation number of central LBGs. We note that for all redshifts and threshold magnitudes shown the mean occupation number of central LBGs plateaus at a value less than unity. Furthermore, the average halo mass of LBGs in any sample varies from 3×10^{11} to $1.5 \times 10^{12}\,{\rm M}_{\odot}$ (see Table 1 and also J13). These galactic dark matter haloes at high-z correspond to 2σ–4σ fluctuations, whereas at $z = 0$ haloes of comparable mass collapse from perturbations that are less than 1σ. Thus, galactic mass dark matter haloes at $z = 4$ are much 'rarer' than those at $z = 0$.

2.2 Analytic model for the non-linear clustering of high-z haloes

Now we briefly describe our model for the non-linear clustering of high-z dark matter haloes on quasi-linear scales. The dark

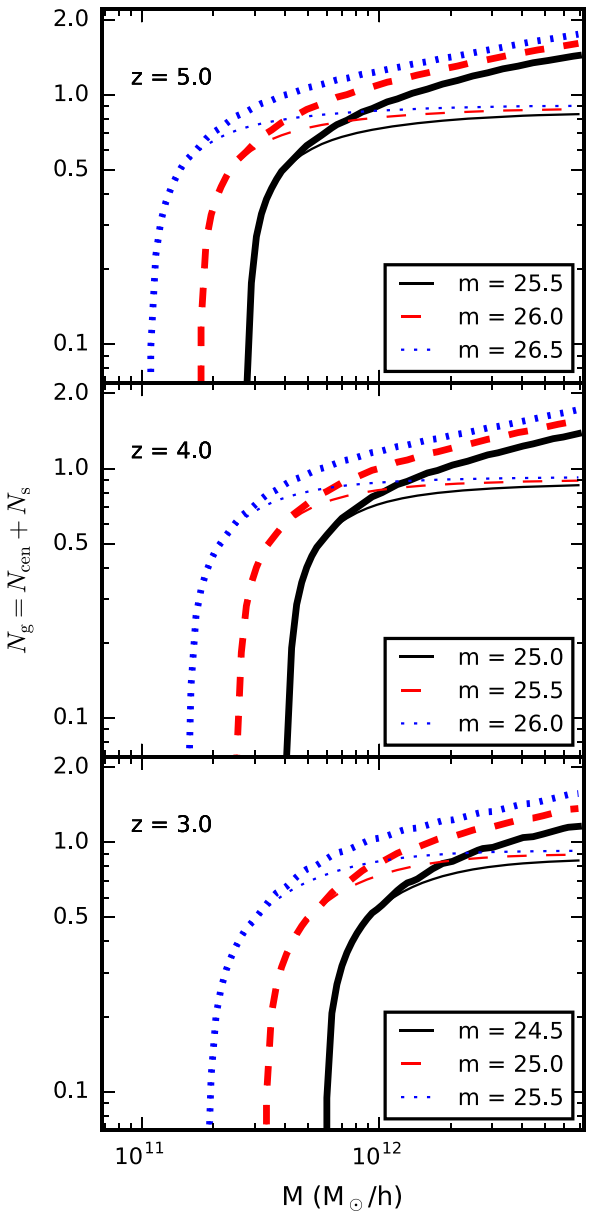

Figure 1. The HOD, $N_g(M, m, z)$, as a function of the mass of the host halo, given by J13 at various redshifts and limiting magnitudes (m) as labelled (same as fig. 7 of J13). In each panel, the thin curves correspond to $N_{cen}(M, m, z)$. The thick curves give the total occupation $N_g(M, m, z) = N_{cen}(M, m, z) + N_s(M, m, z)$. The mean occupation of the central galaxies is always less than unity. For a fuller description see J13.

matter haloes are assumed to be spherical regions with an over-density $\Delta = 200$ times the background density of the Universe. Then, the virial radius r_{200} of any halo of mass M is given by $M = (4/3)\pi r_{200}^3 \rho_c \Delta$. In the linear bias approximation, the cross-correlation between haloes of mass M' and M'' is given by (Cooray & Sheth 2002)

$$\xi_{hh}(r|M', M'', z) = b(M', z)b(M'', z)\xi_{mm}(r, z), \quad (2)$$

where $\xi_{mm}(r, z)$ is the two-point correlation function of the matter density field at redshift z and $b(M, z)$ is the scale-independent linear bias of haloes of mass M. Equation (2) is valid on large scales, where density fluctuations still grow linearly in redshift.

On quasi-linear scales and for rarer haloes, J16 improved the model described in equation (2) by replacing the scale-independent linear halo bias with a scale-dependent non-linear halo bias given by

$$b_{nl}(r, M, z) = b(M, z)\zeta(r, M, z). \quad (3)$$

Here $\zeta(r, M, z)$ is the scale-dependent part of the non-linear halo bias, while $b(M, z)$ is the linear halo bias measured on large scales. The functions $b(M, z)$ and $\zeta(r, M, z)$ are calibrated by fitting to N-body simulations. We also note that, by definition, $\zeta(r, M, z) \longrightarrow 1$ on very large scales.

The expression for the large-scale halo bias $b(M, z)$ is given by the fitting function of Tinker et al. (2010):

$$b(M, z) = b(\nu(M, z)) = 1 - A\frac{\nu^a}{\nu^a + \delta_c^a} + B\nu^b + C\nu^c, \quad (4)$$

where $\nu(M, z) = \delta_c/\sigma(M, z)$ is the peak-height, $\delta_c = 1.686$ is the critical density for spherical collapse and $\sigma(M, z)$ is the linear theory variance of matter fluctuations on a mass scale M at redshift z. J16 found that the Tinker et al. (2010) fitting function slightly over-predicts the large-scale bias of the rarest dark matter haloes. This is probably due to the different algorithms used in these studies to identify dark matter haloes. Therefore, J16 refitted equation (4) finding the best-fitting parameters $A = 1.0$, $a = 0.0906$, $B = -4.5002$, $b = 2.1419$, $C = 4.9148$ and $c = 2.1419$. Here, we will use the parameter values given by J16.

The scale-dependent function $\zeta(r, M, z)$ depends on r, M and z through four quantities: $\nu(M, z)$, $\xi_{mm}(r, z)$, an effective power-law index of $\sigma(M)$, $\alpha_m(z)$, and the matter density of the universe at a given redshift, $\Omega_m(z)$. This effective power-law index, $\alpha_m(z)$, is defined as

$$\alpha_m(z) = \frac{\log(\delta_c)}{\log[M_{nl}(z)/M_{col}(z)]}. \quad (5)$$

Here, M_{nl} is the non-linear mass scale where the peak-height $\nu(M, z) = \delta_c$ ($\sigma(M, z) = 1$) and M_{col} is the collapse mass scale where $\nu(M, z) = 1$ ($\sigma(M, z) = \delta_c$). These masses can be computed numerically for any given cosmological model to evaluate $\alpha_m(z)$. The matter density of the universe at any redshift can be written as

$$\Omega_m(z) = \frac{\Omega_m(0)(1+z)^3}{\Omega_m(0)(1+z)^3 + \Omega_\Lambda(0)}, \quad (6)$$

where $\Omega_m(0)$ and $\Omega_\Lambda(0)$ are the densities of matter and dark energy at $z = 0$ in units of the critical density.

The form for $\zeta(r, M, z)$ expressed in terms of these quantities was found by J16 to be well fitted by

$$\zeta(\xi_{mm}^{sim}, \nu, \alpha_m, \Omega_m(z)) = \left(1 + K_0 \log_{10}\left(1 + {\xi_{mm}}^{k_1}\right) \nu^{k_2}(1 + k_3/\alpha_m)\Omega_m(z)^{k_4}\right) \times \left(1 + L_0 \log_{10}\left(1 + {\xi_{mm}}^{l_1}\right) \nu^{l_2}(1 + l_3/\alpha_m)\Omega_m(z)^{l_4}\right), \quad (7)$$

with $K_0 = 0.1699$, $k_1 = 1.194$, $k_2 = 4.311$, $k_3 = -0.0348$, $k_4 = 17.8283$, $L_0 = 2.9138$, $l_1 = 1.3502$, $l_2 = 1.9733$, $l_3 = -0.1029$ and $l_4 = 3.1731$.

In the top panel of Fig. 2, we plot $\zeta(M, r, z)$ for haloes as a function of separation for three different halo masses that host LBGs at $z = 4$. The bottom panel shows the corresponding non-linear halo bias $b_{nl}(r, M, z)$ of the haloes along with the scale-independent linear halo bias (thin horizontal line) given by equation (4). It is clear from Fig. 2 that $\zeta(M, r, z)$ increases significantly from unity on small scales. As a result, the non-linear halo bias is not constant and is strongly scale-dependent on quasi-linear scales (0.5–10 h^{-1} Mpc). One can see that there is a significant boost in the halo bias at high-z,

Table 1. Column 1: redshift of the galaxy sample; columns 2 and 3: apparent and absolute magnitude limits of the galaxy sample; column 4: mean halo mass of galaxies in the sample as given in J13; columns 5 and 6: the correlation length obtained from the best fitting power law for the linear and non-linear halo bias models; columns 7 and 8: the predicted power-law index of the galaxy correlation function in the range $0.1 \leq r/\mathrm{Mpc} \leq 50$ for the linear and the non-linear halo bias models; and columns 9 and 10: the galaxy bias at 8 h^{-1} Mpc, predicted by the linear and the non-linear halo bias models.

				ξ_g in the range $0.1 \leq r/h^{-1}\mathrm{Mpc} \leq 50$					
				r_0 (Mpc h^{-1})		γ		$b_g = \sqrt{\frac{\xi_g}{\xi_{mm}}}$	
z	m	M_{AB}	$M_{av}/\mathrm{M}_\odot$	Linear	Non-linear	Linear	Non-linear	Linear	Non-linear
	25.5	−21.0	7.0×10^{11}	4.41	7.43	1.55	2.06	5.85	6.53
5	26.0	−20.5	4.5×10^{11}	3.79	6.36	1.53	1.97	5.31	5.80
	26.5	−20.0	2.9×10^{11}	3.25	5.39	1.51	1.89	4.82	5.18
	25.0	−21.1	9.9×10^{11}	4.37	6.71	1.58	1.96	4.72	5.16
4	25.5	−20.6	6.1×10^{11}	3.79	5.72	1.56	1.89	4.29	4.61
	26.0	−20.1	3.9×10^{11}	3.29	4.85	1.54	1.82	3.90	4.14
	24.5	−21.1	1.5×10^{12}	4.26	6.10	1.60	1.93	3.61	3.84
3	25.0	−20.6	9.0×10^{11}	3.67	5.13	1.59	1.86	3.23	4.40
	25.5	−20.1	5.5×10^{11}	3.20	4.36	1.58	1.81	2.92	3.05

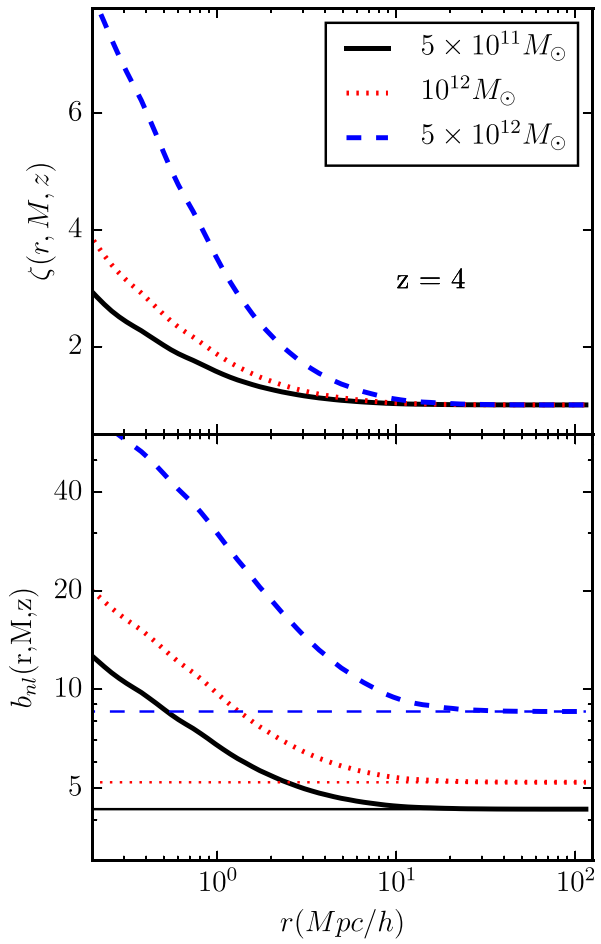

Figure 2. Top panel: the scale dependence $\zeta(r, M, z)$ of the non-linear halo bias as a function of the halo separation for three halo masses at $z = 4$. Bottom panel: the non-linear halo bias (thick lines) $b_{nl}(r, M, z) = b(M, z)\zeta(r, M, z)$ at the same redshift. The thin horizontal lines are the scale-independent linear halo bias $b(M, z)$ for the same masses.

even on scales of $5 - 10\ h^{-1}$ Mpc. For example, at $z = 4$ the bias of dark matter haloes of mass $M = 5 \times 10^{12}\ \mathrm{M}_\odot$ is increased by a factor of 4.5 at a halo separation $r = 1\ h^{-1}$ Mpc, compared to the linear bias of those haloes. This will boost the clustering strength of these haloes by a factor of 20. Furthermore, $\zeta(M, r, z)$ increases with halo mass suggesting that the non-linear bias is stronger for rarer haloes. As we shall see later, such a strong scale-dependent non-linear halo bias results in a remarkable change in the predicted shape of the LBG correlation function compared to the predictions using linear halo bias.

The halo–halo correlation function is then obtained by replacing the linear halo bias with the non-linear halo bias, $b_{nl}(r, M, z)$:

$$1 + \xi_{hh}(r|M', M'', z) = \Big[1 + b_{nl}(r, M', z) b_{nl}(r, M'', z) \times \xi_{mm}(r)\Big]\ \Theta\Big[r - r_{min}(M', M'')\Big] \quad (8)$$

Here, the Θ function incorporates halo exclusion in our calculations. The halo exclusion ensures that the correlation between any pair of haloes of masses M' and M'' goes to -1 if $r < r_{min}(M', M'')$, where $r_{min} = \max[r_{200}(M'), r_{200}(M'')]$ (van den Bosch et al. 2013). Here, $r_{200}(M) = (3M/4\pi\rho_c\Delta)^{1/3}$ is the virial radius of a dark matter halo of mass M with $\Delta = 200$.

3 THE CORRELATION FUNCTIONS OF LBGs

We now incorporate the non-linear halo bias into the halo model of large-scale structure to compute the correlation functions of LBGs. As discussed above, for this we use the HOD (shown in Fig. 1) of LBGs computed using the model of J13. The galaxy correlation functions have a contribution from the two-halo term that describe the clustering between galaxies hosted in distinct haloes and a one-halo term that accounts for the clustering from galaxies residing in the same dark matter halo. The non-linear halo bias modifies, the two-halo term by boosting the clustering of galaxies on quasi-linear scales. The one-halo term, however, remains unchanged because the non-linear halo bias does not alter the distribution of galaxies inside a dark matter halo.

3.1 The two-halo term

When computing the two-halo term with non-linear halo bias, we assume that the halo density profile is sufficiently peaked that it does not affect the two-halo term on scales larger than the typical virial radii of haloes (Cooray & Sheth 2002). This is equivalent to assuming that the halo density profile is a delta function when

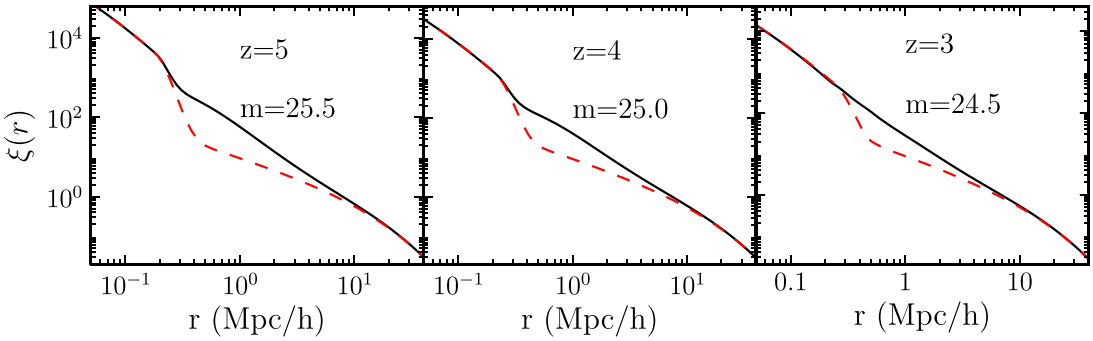

Figure 3. The spatial correlation functions, ξ_g, of high-z LBGs at redshifts 3, 4 and 5 and for a given apparent magnitude limit as labelled. The red dashed and black solid curves are the predictions of scale-independent linear halo bias and scale-dependent non-linear halo bias models, respectively.

computing the two halo term.[1] In this case, using equation (8), the two-halo term for galaxy correlation function can be written as

$$1+\xi_g^{2h}(r,m,z)=\frac{1}{n_g(m,z)}\int dM'\frac{dn}{dM}(M')N_g(M',m,z)\times\int dM''\frac{dn}{dM}(M'')N_g(M'',m,z)\left[1+\xi_{hh}(r|M',M'',z)\right], \quad (9)$$

where

$$n_g(m,z)=\int dM\frac{dn}{dM}(M,z)N_g(M,m,z) \quad (10)$$

is the number density of LBGs brighter than apparent magnitude m given by equation (1). We use the fitting function of Tinker et al. (2008) for the halo mass function, $dn/dM(M,z)$, as this is found to be in excellent agreement with the halo mass function measured from N-body simulations, which is used to calibrate the non-linear halo bias. We have also incorporated the halo exclusion in equation (9) through the Θ function in equation (8).

3.2 The one-halo term

The one-halo term is computed as in J13, assuming that the radial distribution of satellite galaxies inside a parent halo follows the dark matter density distribution (Cooray & Sheth 2002). We use the Navarro–Frenk–White (NFW) profile for the density distribution in a dark matter halo (Navarro, Frenk & White 1997). The halo concentration parameter for computing NFW fitting functions is taken from Klypin, Trujillo-Gomez & Primack (2011). In this case, the one-halo term is given by (Sheth et al. 2001; Tinker et al. 2005)

$$\xi_g^{1h}(r,m,z)=\frac{1}{n_g^2}\int dM\,\frac{dn}{dM}(M,z)\times\left[2N_{cen}(M,m,z)\times N_s(M,m,z)\frac{\rho_{NFW}(r,M,z)}{M}+N_s{}^2(M,m,z)\rangle\frac{\lambda_{NFW}(r,M,z)}{M^2}\right]. \quad (11)$$

Here, ρ_{NFW} is the NFW profile of dark matter density inside a collapsed halo and λ_{NFW} is the convolution of this density profile with itself (Sheth et al. 2001).

[1] We found that this approximation is sufficient to study the clustering of LBGs.

3.3 The total spatial correlation function

The galaxy correlation function is obtained by adding the one-halo and the two-halo terms

$$\xi_g(r,m,z)=\xi^{1h}(r,m,z)+\xi^{2h}(r,m,z). \quad (12)$$

In Fig. 3, we show the predicted spatial correlation functions of LBGs at $z=3$, 4 and 5. Each panel corresponds to a given redshift and threshold apparent magnitude. Fig. 3 clearly shows that, at each redshift, the linear halo bias model prediction for ξ_g breaks away from a power law on scales from 0.1 to $10\,h^{-1}$ Mpc. On similar scales, the non-linear halo bias model predicts much stronger clustering compared to the linear halo bias model. As a result, the deviation of ξ_g from a power law with the non-linear halo bias model is far smaller than is the case for the linear halo bias model. We also find that the discrepancy between the predictions of the two models increases with redshift and luminosity. In fact, it is clear from Fig. 3 that, at $z=5$, the linear halo bias model underpredicts the correlation functions by more than an order of magnitude in the range $0.5 \le r/(h^{-1}\,\mathrm{Mpc}) \le 1$ compared to the non-linear halo bias model. This clearly shows that the non-linear bias of dark matter haloes must be properly accounted for in order to understand the clustering of high-z galaxy samples that are characterized by low number densities.

We have fitted the $\xi_g(r)$ predicted by the linear and non-linear halo bias models with a power law $\xi_g(r)=(r/r_0)^{-\gamma}$, where r_0 is the correlation length and γ is the power-law index. The best-fitting r_0 and γ, obtained by fitting ξ_g in the range $0.1 \le r/h^{-1}\,\mathrm{Mpc} \le 50$, are tabulated in Table 1. It is clear from columns 5 and 6 of Table 1 that the correlation lengths predicted by the non-linear halo bias model are systematically higher than those obtained from the linear halo bias model. This is a direct consequence of the increased clustering of LBGs on quasi-linear scales in the non-linear halo bias model. In particular, for the brightest LBG sample at $z=5$, the predicted correlation length in the non-linear halo bias model is larger by a factor of 1.7 compared to the linear bias prediction. Furthermore, r_0 increases with redshift and galaxy luminosity. For example, the correlation length at $z=5$ is larger by a factor of $\sim$1.2 compared to that at $z=3$ for a given apparent limiting magnitude. This is consistent with the observational results of Hildebrandt et al. (2009), who found a similar evolution of r_0 with redshift and limiting magnitude.

The power-law slopes of the predicted ξ_g for the linear and the non-linear bias models are given in columns 7 and 8 of Table 1. It is clear from Table 1 that, the linear halo bias model predicts $\gamma = 1.5$–1.6. On the other hand, γ predicted by non-linear and

scale-dependent bias model ranges typically from 1.8–2.1. This is remarkably consistent with the values of the power-law index ($\gamma \sim 1.7$–2.1) inferred from high-redshift observations (Ouchi et al. 2005; Lee et al. 2006; Coil et al. 2006; Hildebrandt et al. 2009; Savoy et al. 2011; Bian et al. 2013; Barone-Nugent et al. 2014; Durkalec et al. 2015; Harikane et al. 2016).

Finally, we compare the galaxy bias predicted on large scales by the linear and non-linear models. We first note that the large-scale LBG bias has been measured by numerous authors at different scales using alternative definitions. Several set the scale at which the bias of LBGs is measured to be 8 h^{-1} Mpc (Ouchi et al. 2004; Adelberger et al. 2005; Yoshida et al. 2008; Hildebrandt et al. 2009). Following these, we have defined the galaxy bias, $b_{\rm g}$ at a scale of 8 h^{-1} Mpc as

$$b_{\rm g} = \sqrt{\frac{\xi_{\rm g}(r)}{\xi_{\rm mm}(r)}}\Bigg|_{r=8\,h^{-1}\,{\rm Mpc}} \quad (13)$$

The galaxy bias estimated using equation (13) for the linear and non-linear bias models are tabulated in columns 9 and 10 of Table 1, respectively. Interestingly, we find that $b_{\rm g}$ predicted by the non-linear halo bias model are consistently higher than the linear halo bias predictions. Specifically, in the redshift range 3–5, the galaxy bias is larger by 4–12 per cent in the non-linear halo clustering model compared to the linear halo bias model. It is remarkable that the non-linear dark matter halo clustering results in such an increment in the galaxy bias even on a scale of 8 h^{-1} Mpc at high-z where matter fluctuations are still in the linear regime.[2]

3.4 The angular correlation function

Now we compute the angular correlation function, a direct measurable of galaxy clustering, from the spatial correlation function. Several authors have measured the angular correlation function of LBGs brighter than a given UV luminosity in the redshift range $3 \leq z \leq 5$ (Ouchi et al. 2005; Coil et al. 2006; Kashikawa et al. 2006; Lee et al. 2006; Hildebrandt et al. 2009; Savoy et al. 2011; Wake et al. 2011; Bian et al. 2013; Barone-Nugent et al. 2014; Durkalec et al. 2015; Harikane et al. 2016). Among these studies, Hildebrandt et al. (2009) use the largest LBG sample in the redshift range $3 \leq z \leq 5$. This allows them to estimate the angular correlation functions with small error bars for a range of magnitudes. Hence, we will use the Hildebrandt et al. (2009) data when comparing our model predictions with observations.

The luminosity-dependent angular correlation function $w(\theta, m, z)$ is computed from the spatial correlation function using Limber's equation (Peebles 1980):

$$w(\theta, m, z) = \int_0^\infty {\rm d}z'\, N(z') \int_0^\infty {\rm d}z''\, N(z'') \xi_{\rm g}\left(z, r(\theta; z', z'')\right), \quad (14)$$

where $r(\theta; z', z'')$ is the comoving separation between two points at z' and z'' subtending an angle θ with respect to an observer. To compute the angular correlation functions, we used the normalized redshift selection function, $N(z)$, from Hildebrandt et al. (2009) ($BC_{\rm sim}$ redshift distribution; see table 4 and fig. 5 of their paper). Furthermore, in equation (14), the spatial two-point correlation function $\xi_{\rm g}(r, z)$ is always evaluated at the central redshift of the selection function $N(z)$.

[2] For example, $\sigma_8 = 0.175$ at $z = 5$.

In Fig. 4, we show in solid black lines, the angular correlation functions of high-z LBGs computed after incorporating the non-linear halo bias. The results are presented for $3 \leq z \leq 5$ and for a wide range of magnitude limits. Fig. 4 also shows the angular correlation function of LBGs computed using the linear halo bias model given in J13 as dashed red lines.

First, we note that the clustering predictions using linear halo bias compare reasonably well with the observed data for $\theta > 100$ arcsec. However, on intermediate angular scales ($5 \leq \theta \leq 100$ arcsec), the linear halo bias predictions do not match the observed clustering. Here, there is a clear break in the predicted angular correlation functions around $\theta \sim 10$ arcsec, due to which the correlation functions look like a double power law. This scale corresponds to the transition from the two-halo to one-halo contributions to the clustering. Furthermore, the discrepancy between theory and observations seems to increase for brighter and higher-z galaxy samples.

The strong feature in the predicted LBG clustering at intermediate angular scales can also be found in earlier studies using the halo model (Hamana et al. 2004; Ouchi et al. 2005; Lee et al. 2009; Bian et al. 2013; J13; Harikane et al. 2016). These studies use the linear halo bias model for the two-halo contribution, which, in turn, results in a very strong deviation of the predicted angular correlation function from a power law. It is possible to increase the clustering strength over the range $5 \leq \theta \leq 100$ arcsec by changing the HOD given by $N_{\rm g}$ in equation (9). However, this will simply rescale $\xi_{\rm g}$ upwards and as a result, on large scales, the linear halo bias model will overpredict the observed clustering.

Our model predictions using non-linear halo bias significantly increase the clustering strength of LBGs only in the angular range $5 \leq \theta \leq 100$ arcsec, on the whole greatly improving the agreement with observational measurements. It is also clear that the boost in the clustering strength due to the non-linear halo bias on this scale is larger for higher redshift and for brighter galaxy samples. As a result, the feature predicted by the linear halo bias model at the two-halo to one-halo transition region (at $\theta \sim 10$ arcsec), weakens and the correlation function is closer to a power law. Therefore, we conclude that the non-linear bias of high-z dark matter haloes plays a major role in reshaping the correlation functions of high-z galaxies, thereby providing better agreement with the observational data.

We also note from Fig. 4 that, for fainter galaxy samples ($m = 25.0$ and 25.5) at $z = 3$, the non-linear bias model slightly overpredicts the clustering on intermediate angular scales, and the linear bias model provides a better fit to the data. One could, in principle, investigate whether this is due to uncertainties in the HODs of those samples by using alternative HODs derived from more sophisticated galaxy formation models, but such an analysis is beyond the scope of this paper. However, apart from these two cases, the clustering measurements for all of the other galaxy samples are much better fit by the non-linear halo bias model than the linear halo bias model.

Finally, it is clear from Fig. 4 that, on scales smaller than $\sim$10 arcsec and larger than $\sim$100 arcsec, the correlation functions of LBGs, as predicted by linear and non-linear halo bias models, agree well with each other. As noted earlier, for $\theta \leq 10$ arcsec, the non-linear halo bias does not affect the correlation function because the clustering on these scales is dominated by the one-halo contribution due to pairs of galaxies sitting inside the same dark matter halo. On the other hand, on large scales $\zeta(r, M, z) \rightarrow 1$ and hence the expression for the non-linear halo bias in equation (3) reduces back to the linear halo bias. As a result, for $\theta \geq 100$ arcsec, the effect of scale-dependent non-linear bias is insignificant for LBG clustering.

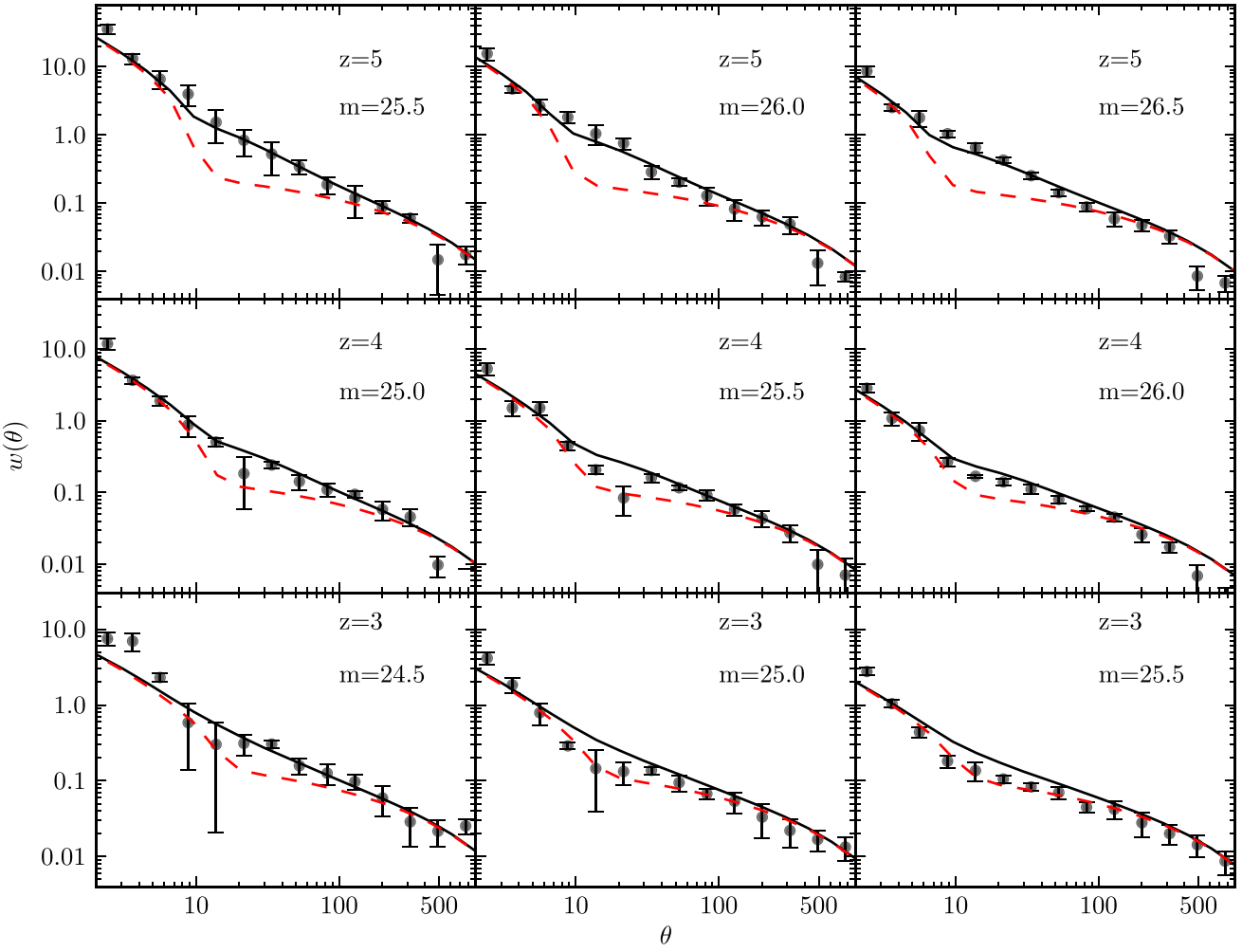

Figure 4. The angular correlation functions of LBGs predicted using non-linear (solid black) and linear (dashed red) halo bias models at redshifts 3, 4 and 5 and for various limiting magnitudes as labelled. In each row there are three panels showing the clustering predictions of LBGs samples with three apparent magnitude limits. The observational clustering measurements are taken from Hildebrandt et al. (2009)

4 DISCUSSION AND CONCLUSIONS

We have investigated the non-linear clustering of high-z LBGs in the redshift range $3 \leq z \leq 5$ using the halo model of large- scale structure. Specifically, we find that incorporating the non-linear halo bias of these haloes in the halo model is of utmost importance for understanding the clustering of LBGs in the quasi-linear regime corresponding to angular scales of $5 \leq \theta \leq 100$ arcsec.

Our work is motivated by J13, who showed that the halo model predictions using linear halo bias for halo clustering fail to explain the observed clustering amplitude of LBGs at $3 \leq z \leq 5$ on angular scales $5 \leq \theta \leq 100$ arcsec. The linear halo bias models underpredict LBG clustering on these scales by an order of magnitude. As a result, the predicted LBG correlation functions in the above redshift range depart significantly from a power law in contrast with observations.

We address this issue using the model of J16, who investigated the non-linear clustering of high-z dark matter haloes in the redshift range and on the scales of interest. In particular, these authors provide an analytic fitting function for the scale-dependent non-linear halo bias of high-z haloes on quasi-linear scales, which is a function of four quantities that can be readily computed for any cosmology. Using this, we find that, at $z = 4$, the non-linear bias of dark matter haloes of mass $\sim 10^{12}\,\mathrm{M}_{\odot}$, that host typical LBGs at this redshift, is quite significant on quasi-linear scales. As a result, the clustering amplitude is enhanced by up to a factor of 20 at a scale of 0.5 h^{-1}Mpc.

We combined the analytic fitting formula for non-linear halo bias given by J16 with the halo model to predict the spatial correlation function of LBGs. For this we used the HOD of LBGs given by J13, computed using their galaxy formation model. The corresponding predicted correlation function shows much stronger clustering on scales 0.1–10 h^{-1} Mpc compared to the predictions of the linear halo bias model. Furthermore, the difference between the models increases with redshift and galaxy luminosity. The resulting galaxy correlation function in the non-linear halo bias model are much closer to a power law than the predictions of the linear halo bias model. The corresponding correlation lengths of LBGs are consistently larger in the non-linear halo bias model compared to the linear halo bias model. For example, at $z = 5$ and for a limiting magnitude of $m = 25.5$, the predicted correlation length in the non-linear halo bias model is larger than the linear halo bias model by 70 per cent. Moreover, the non-linear halo bias model predicts a power-law index of $\gamma \sim 1.8$–2.1 compared to $\gamma \sim 1.5$–1.6 obtained from the linear halo bias model. Remarkably, the power-law index estimated

using the non-linear halo bias model at high redshifts compares very well with the values deduced from several high-redshift observations.

The spatial correlation functions are then used to compute the angular correlation functions of LBGs. We find that the non-linear bias of dark matter haloes significantly boosts the clustering of LBGs on angular scales of interest ($10 \leq \theta \leq 100$ arcsec). The resulting LBG correlation functions provide a much better fit to the observed data on these angular scales compared to the predictions of the linear halo bias model, except for the fainter galaxy samples at $z = 3$. The effect of non-linear halo clustering is also found to increase with redshift and galaxy luminosity. This is expected because the non-linear bias is larger for more massive and higher redshift dark matter haloes. This, in turn, reshapes the angular correlation functions of LBGs in the redshift range 3–5 into an approximate power law over the entire angular scale. While at low-z, a power law $\xi_{\rm g}(r)$ is achieved by the fine-tuning of several ingredients including the HOD and the dark matter clustering (Watson et al. 2011), we believe at high-z the non-linear halo bias plays a critical role in making the shape of the galaxy correlation function close to a power law.

Finally, the predicted LBG bias at 8 h^{-1} Mpc is larger in the non-linear halo bias model compared to the linear halo bias predictions for all redshifts and limiting magnitudes. In particular, for $3 \leq z \leq 5$, we find a 4–12 per cent increase in the galaxy bias on this scale in the non-linear halo clustering models. This is because the effective bias on this scale is not the linear asymptotic bias, but is still subject to a substantial scale-dependent effect, as shown by Fig. 2. Since several studies measure the galaxy bias of LBGs at 8 h^{-1} Mpc (Ouchi et al. 2004; Adelberger et al. 2005; Yoshida et al. 2008; Hildebrandt et al. 2009), it is very important to include the non-linear halo bias in the halo model of LBG clustering for a reliable comparison of data and theory.

The observed clustering of LBGs has been used in numerous studies as a probe of the physics of high-redshift galaxy formation (Hamana et al. 2004, Ouchi et al. 2005, Lee et al. 2009, Ouchi et al. 2010, Bian et al. 2013, Cooke, Omori & Ryan-Weber 2013, Jose, Srianand & Subramanian 2013a; Durkalec et al. 2015; Harikane et al. 2016). These studies used the linear halo bias model to place constraints on several interesting quantities such as the average mass of haloes hosting LBGs, the duty cycle of star formation activity and the fraction of satellite galaxies at high redshifts. The use of the linear halo bias model potentially introduces systematics in the inferred values of these quantities. For example, for LBGs brighter than $m = 26.5$ at $z = 5$, focusing on just the measured galaxy clustering at $\theta \sim 14$ arcsec rather than the whole correlation function (see Fig. 4), comparing to the clustering expected in the dark matter suggests a galaxy bias of $b_{\rm g} \sim 9.3$. In the linear model, this bias translates into a mean halo mass of $\sim 4.2 \times 10^{12}$ M$_\odot$. However, if instead we use the non-linear halo bias model to interpret the clustering at this fixed angular scale, part of the difference in amplitude between the galaxy clustering and the dark matter clustering is due to the non-linear effects. This means that the asymptotic bias on large scales is smaller than in the linear halo bias model, implying a lower mean halo mass $\sim 3.9 \times 10^{11}$ M$_\odot$, which is an order of magnitude smaller than that inferred from the linear halo bias model. Therefore, it is very important to incorporate the non-linear halo bias of high-z haloes in the clustering models of LBGs to better explore the physics of galaxy formation and cosmology.

Even though we have focused on the importance of the non-linear halo bias for the clustering of LBGs at $3 \leq z \leq 5$, one can expect similar trends in the clustering of rare, high-redshift galaxies for other sample selections. In particular, strongly non-linear clustering is expected for high-z quasars, Lyman-α emitters, dusty star-forming galaxies and redshifted 21 cm signals from the pre-reionization era. The extended version of the halo model, we have introduced that incorporates the non-linear bias of dark matter haloes will be a useful tool for the robust interpretation of such measurements.

ACKNOWLEDGEMENTS

CJ acknowledges a Durham COFUND Junior Research Fellowship (4958) supported by the DIFeREns2 project that has received funding from the European Union's Seventh Framework Programme for research, technological development and demonstration under grant agreement no 609412. This work was supported by the Science and Technology Facilities Council [ST/L00075X/1]. This work used the DiRAC Data Centric System at Durham University, operated by the ICC on behalf of the STFC DiRAC HPC Facility (www.dirac.ac.uk). This equipment was funded by BIS National E-infrastructure capital grant ST/K00042X/1, STFC capital grant ST/H008519/1, and STFC DiRAC Operations grant ST/K003267/1 and Durham University. DiRAC is part of the UK's National E-Infrastructure.

REFERENCES

Adelberger K. L., Steidel C. C., Pettini M., Shapley A. E., Reddy N. A., Erb D. K., 2005, ApJ, 619, 697
Barone-Nugent R. L. et al., 2014, ApJ, 793, 17
Berlind A. A., Weinberg D. H., 2002, ApJ, 575, 587
Bian F. et al., 2013, ApJ, 774, 28
Bond J. R., Cole S., Efstathiou G., Kaiser N., 1991, ApJ, 379, 440
Bouwens R. J., Illingworth G. D., Franx M., Ford H., 2007, ApJ, 670, 928
Bouwens R. J. et al., 2012, ApJ, 752, L5
Bullock J. S., Wechsler R. H., Somerville R. S., 2002, MNRAS, 329, 246
Coil A. L., Newman J. A., Cooper M. C., Davis M., Faber S. M., Koo D. C., Willmer C. N. A., 2006, ApJ, 644, 671
Cole S., Kaiser N., 1989, MNRAS, 237, 1127
Conroy C., Wechsler R. H., Kravtsov A. V., 2006, ApJ, 647, 201
Cooke J., Omori Y., Ryan-Weber E. V., 2013, MNRAS, 433, 2122
Cooray A., 2004, MNRAS, 348, 250
Cooray A., Ouchi M., 2006, MNRAS, 369, 1869
Cooray A., Sheth R., 2002, Phys. Rep., 372, 1
Durkalec A. et al., 2015, A&A, 583, A128
Guo H. et al., 2013, ApJ, 767, 122
Hamana T., Ouchi M., Shimasaku K., Kayo I., Suto Y., 2004, MNRAS, 347, 813
Hamana T., Yamada T., Ouchi M., Iwata I., Kodama T., 2006, MNRAS, 369, 1929
Harikane Y. et al., 2016, ApJ, 821, 123
Hildebrandt H., Pielorz J., Erben T., van Waerbeke L., Simon P., Capak P., 2009, A&A, 498, 725
Hinshaw G. et al., 2013, ApJS, 208, 19
Iliev I. T., Scannapieco E., Martel H., Shapiro P. R., 2003, MNRAS, 341, 81
Ishikawa S., Kashikawa N., Toshikawa J., Tanaka M., Hamana T., Niino Y., Ichikawa K., Uchiyama H., 2016, preprint (arXiv:1612.06869)
Jose C., Srianand R., Subramanian K., 2013a, MNRAS, 435, 368
Jose C., Subramanian K., Srianand R., Samui S., 2013b, MNRAS, 429, 2333 (J13)
Jose C., Lacey C. G., Baugh C. M., 2016, MNRAS, 463, 270 (J16)
Kaiser N., 1984, ApJ, 284, L9
Kashikawa N. et al., 2006, ApJ, 637, 631
Klypin A. A., Trujillo-Gomez S., Primack J., 2011, ApJ, 740, 102
Kravtsov A. V., Berlind A. A., Wechsler R. H., Klypin A. A., Gottlöber S., Allgood B., Primack J. R., 2004, ApJ, 609, 35
Lacey C., Cole S., 1993, MNRAS, 262, 627

Lee K.-S., Giavalisco M., Gnedin O. Y., Somerville R. S., Ferguson H. C., Dickinson M., Ouchi M., 2006, ApJ, 642, 63
Lee K.-S., Giavalisco M., Conroy C., Wechsler R. H., Ferguson H. C., Somerville R. S., Dickinson M. E., Urry C. M., 2009, ApJ, 695, 368
Mo H. J., White S. D. M., 1996, MNRAS, 282, 347
Navarro J. F., Frenk C. S., White S. D. M., 1997, ApJ, 490, 493
Ouchi M. et al., 2004, ApJ, 611, 685
Ouchi M. et al., 2005, ApJ, 635, L117
Ouchi M. et al., 2010, ApJ, 723, 869
Parejko J. K. et al., 2013, MNRAS, 429, 98
Park J., Kim H.-S., Wyithe J. S. B., Lacey C. G., Baugh C. M., Barone-Nugent R. L., Trenti M., Bouwens R. J., 2016, MNRAS, 461, 176
Peebles P. J. E., 1980, The Large-Scale Structure of the Universe. Princeton Univ Press, Princeton, NJ
Reddy N. A., Steidel C. C., Pettini M., Adelberger K. L., Shapley A. E., Erb D. K., Dickinson M., 2008, ApJS, 175, 48
Reed D. S., Bower R., Frenk C. S., Jenkins A., Theuns T., 2009, MNRAS, 394, 624
Samui S., Srianand R., Subramanian K., 2007, MNRAS, 377, 285
Savoy J., Sawicki M., Thompson D., Sato T., 2011, ApJ, 737, 92
Seljak U., 2000, MNRAS, 318, 203
Sheth R. K., Tormen G., 1999, MNRAS, 308, 119
Sheth R. K., Hui L., Diaferio A., Scoccimarro R., 2001, MNRAS, 325, 1288
Tinker J. L., Weinberg D. H., Zheng Z., Zehavi I., 2005, ApJ, 631, 41
Tinker J., Kravtsov A. V., Klypin A., Abazajian K., Warren M., Yepes G., Gottlöber S., Holz D. E., 2008, ApJ, 688, 709
Tinker J. L., Robertson B. E., Kravtsov A. V., Klypin A., Warren M. S., Yepes G., Gottlöber S., 2010, ApJ, 724, 878
van den Bosch F. C., More S., Cacciato M., Mo H., Yang X., 2013, MNRAS, 430, 725
Wake D. A. et al., 2011, ApJ, 728, 46
Watson D. F., Berlind A. A., Zentner A. R., 2011, ApJ, 738, 22
Yoshida M., Shimasaku K., Ouchi M., Sekiguchi K., Furusawa H., Okamura S., 2008, ApJ, 679, 269
Zehavi I. et al., 2004, ApJ, 608, 16
Zehavi I. et al., 2005, ApJ, 630, 1
Zehavi I. et al., 2011, ApJ, 736, 59
Zheng Z. et al., 2005, ApJ, 633, 791
Zheng Z., Zehavi I., Eisenstein D. J., Weinberg D. H., Jing Y. P., 2009, ApJ, 707, 554

This paper has been typeset from a TEX/LATEX file prepared by the author.